Electronic Supplementary Material (ESI) for Chemical Communications.
This journal is © The Royal Society of Chemistry 2018

Layer-sliding-driven crystal size and photoluminescence change in a novel SCC-MOF

Xiang-Sha Du[a], Bing-Jie Yan[a], Jia-Yin Wang[a], Xiao-Juan Xi[a], Zhao-Yang Wang[*a],

Shuang-Quan Zang[*a]

[a]*College of Chemistry and Molecular Engineering, Zhengzhou University, Zhengzhou 450001, China*

*E-mail: zangsqzg@zzu.edu.cn

wangzy@zzu.edu.cn

Materials and Methods

Materials and reagents

All reagents and solvents used were of commercially available reagent grade and were used without any additional purification.

Characterization

^{1}H NMR was carried out on a Bruker 400 spectrometer. Thermogravimetric (TG) analyses of the compounds were performed on a SDT 2960 thermal analyzer from room temperature to 400 ℃ at a heating rate of 10 ℃/min under N_2 atmosphere. Elemental Analysis(EA) were carried out at on a FLASH EA 112 elemental analyzer.

Powder X-ray diffraction (PXRD)

PXRD patterns of the compounds were collected at room temperature in air on a X'Pert PRO diffractometer (Cu-Kα). PXRD data for those with mother liquid were collected using Bruker D8 Advance diffractometer (Cu-Kα), during which the samples were packed and sealed in glass capillary with a small quantity of mother liquid.

Single-crystal X-ray diffraction (SCXRD) measurements and details for structure determination

Single-crystal X-ray diffraction measurements of **Ag_{12}TPPA·AA**, **Ag_{12}TPPA·AB** and **Ag_{12}TPPA·ABC_250 K** were performed on a Rigaku XtaLAB Pro diffractometer with Cu-Kα radiation (λ = 1.54178 Å) at 250 K and **Ag_{12}TPPA·ABC_100 K** was measured with Mo-Kα radiation (λ = 0.71073 Å) at 100 K. Data collection and reduction were performed using the program CrysAlisPro[1]. The intensities were corrected for absorption using empirical method implemented in SCALE3 ABSPACK scaling algorithm[2]. The structures were solved with intrinsic phasing methods (*SHELXT-2015*[3]) for **Ag_{12}TPPA·AB**, direct methods (*SHELX*[4]) for **Ag_{12}TPPA·AA** and **Ag_{12}TPPA·ABC**, and refined by full-matrix least squares on F^2 using *OLEX2*,[5] which utilizes the *SHELXL-2015* module.[6] For each of the three structures, all hydrogen atoms were assigned isotropic displacement coefficients U(H) = 1.2U or 1.5U and their coordinates were allowed to ride on their respective atoms, and all non-hydrogen atoms, including the disordered fragments were located in difference-Fourier maps, and refined anisotropically. CF_3COO^-, $-S^tBu$ and the silver atoms they coordinated all suffered positional disorder because of the lattice symmetry

with fixed occupancy. CF_3COO^- and $-S^tBu$ both located at the same position but can't co-exist. Therefore, the PART instruction was used to divide them into two groups. The F atoms of the CF_3COO^- are in two orientations located with equal occupancies. The benzene and pyridine rings of the TPPA molecules were also found to be disordered over two sites with the fixed occupancy of 0.5. The least-squares refinement of the structural model was performed under hard geometry restraints and displacement parameter restrains, such as SADI, ISOR, EADP and EXYZ for the CF_3COO^-, $-S^tBu$ and TPPA molecule. In addition, modeling of electron density within the voids of the frameworks did not lead to identification of guest (DMAc) entities in structures, which is due to the seriously disorder arising from the quite weak interaction between guest and the host framework as well as the high lattice symmetry. Thus the remaining electron density was flattened out using the solvent masking protocol inside *OLEX2* which results in a decrease in the final R value. The information of the crystal data and refinement results for all compounds are summarized in Supplementary Table 1.

Calculation of void space

The fraction of void space was calculated from X-ray structural data of **Ag_{12}TPPA** by PLATON: The unit cell is filled with the atoms from the structural model and each specific atom is assigned its respective van der Waals radius. A grid search generates a list of grid points with a minimum distance of 1.2 Å from the nearest van der Waals surface. This list of grid points is then used to produce a new list of grid points that makes up the solvent accessible areas. For the sets of grid points, the center of gravity and volume of the void are calculated. The overall solvent accessible volume is calculated along with the volume and center of gravity of individual 'voids'.

Luminescence decay measurements

Luminescence microscopy images were recorded on an Olympus BX 53 microscope, and measurements were carried out using a HORIBA FluoroLog-3 fluorescence spectrometer. Steady-state photoluminescence (PL) spectroscopy, emission decay spectroscopy and time-resolved emission spectroscopy (TRES) were performed on a HORIBA FluoroLog-3 spectrofluorometer equipped with an East Changing TC202 temperature controller; the spectra were recorded using the time-correlated single-photon counting (TCSPC) method. Before measurement of temperature-dependent steady and transient luminescence, **Ag_{12}TPPA·AA** were first loaded into

the temperature-controlled instrument with each border of the sample cell sealed by vaseline in case of the solvent escaping and then evacuated for 30 min using a VALUE VRD-16 vacuum pump.

SEM measurements

Scanning electron microscopy (SEM) measurement was carried out using ZeissSigma 500.

Synthesis of Ag_{12}TPPA·AA: AgS^tBu was prepared from the reaction of Ag_2O and HS^tBu in Et_3N. The ligand TPPA was synthesized through Suzuki coupling of tris(4-iodophenyl)amine and pyridine-4-boronic acid according to a reported protocol.[7] In a typical reaction, addition of CF_3COOAg (0.045 g, 0.2 mmol) to a DMAc (dimethylacetamide) solution of AgS^tBu (0.06 g, 0.3 mmol) under stirring gave a colorless clear solution, which was then heated to 40 ℃ followed by droplet addition of DMAc solution of TPPA (0.015 g, 0.3 mmol). Hexagon colorless crystals of **Ag_{12}TPPA·AA** were obtained in minutes. (Yield：94.8 % based on TPPA).

Elemental Analysis: Ag_{12}TPPA·AB ($C_{102}H_{102}Ag_{12}F_{18}N_8O_{12}S_6$·1.7DMAc: calc.(%) C 36.21, N 3.76, H 3.27; found C 36.45, N 3.48, H 3.36). **Ag_{12}TPPA·ABC** ($C_{102}H_{102}Ag_{12}F_{18}N_8O_{12}S_6$·0.9DMAc: calc.(%) C 35.83, N 3.52, H 3.13; found C 35.44, N 3.63, H 3.31).

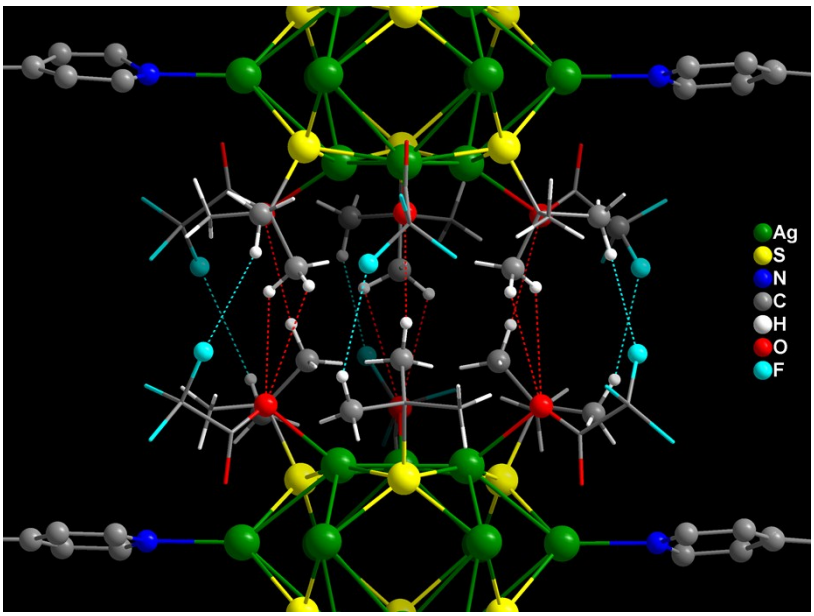

Figure S1. The C–H···F weak interactions between –S^{t}Bu and CF_3COO^- among adjacent layers (turquoise dash line) with the H···F distances (C–H···F angles) are 2.691 Å (154.6°) and 2.960 Å (153.7°), respectively. The C–H···O weak interaction between ^{t}BuS$^-$ and CF_3COO^- among

adjacent layers (red dash line), the H···O distances (C–H···O angles) are 2.751 Å (170.2°), 2.847 Å (116.5°) and 3.060 Å (101.7°), respectively.

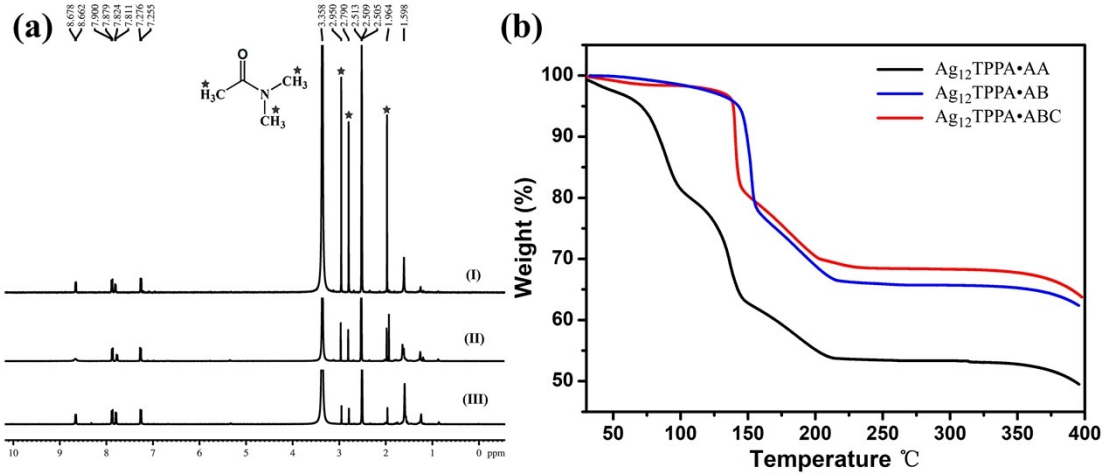

Figure S2. (a) ^{1}H NMR (DMSO-d_6, 400 MHz) spectra of newly obtained **Ag_{12}TPPA·AA** under different treatments: (I) rapidly dissolved in DMSO-d_6; (II) exposed to air for 10 hours to allow the DMAc within the channel freely volatilize before dissolving in DMSO-d_6; (III) stayed in mother liquid for 24 hours and then freely volatilize for 10 hours and dissolved in DMSO-d_6. **Ag_{12}TPPA·AA**, **Ag_{12}TPPA·AB**, **Ag_{12}TPPA·ABC** contain 8, 1.7 and 0.9 DMAc molecules corresponding to each Ag_{12} cluster, respectively. (b) The TGA curves for **Ag_{12}TPPA·AA**, **Ag_{12}TPPA·AB**, **Ag_{12}TPPA·ABC** under N_2 atmosphere (10 ℃/min). **Ag_{12}TPPA·AB** and **Ag_{12}TPPA·ABC** display a 4% and 2% weight loss corresponding to about 1.7 and 0.9 DMAc molecules, respectively, up to 135 and 125 ℃.

Table S1. Crystal data and structure refinement for **Ag_{12}TPPA**

	Ag_{12}TPPA·AA	**Ag_{12}TPPA·AB**	**Ag_{12}TPPA·ABC _100 K**	**Ag_{12}TPPA·ABC _250 K**
CCDC number	1824599	1824600	1824601	1838539
Empirical formula	$C_{102}H_{102}Ag_{12}F_{18}N_8O_{12}S_6$	$C_{102}H_{102}Ag_{12}F_{18}N_8O_{12}S_6$	$C_{102}H_{102}Ag_{12}F_{18}N_8O_{12}S_6$	$C_{102}H_{102}Ag_{12}F_{18}N_8O_{12}S_6$
Formula weight	3460.71	3460.71	3460.71	3460.71
Temperature / K	250.00(10)	250.00(10)	100.00(10)	250.00(10)
Crystal system	trigonal	hexagonal	trigonal	trigonal
Space group	P-3	$P6_3/mmc$	R-3m	R-3m
a /Å	43.8008(6)	25.2076(4)	25.0204(7)	25.140(3)
b /Å	43.8008(6)	25.2076(4)	25.0204(7)	25.140(3)
c /Å	11.1753(4)	15.3459(3)	19.7901(12)	20.039(4)
α /°	90	90	90	90
β /°	90	90	90	90
γ /°	120	120	120	120
Volume /Å^3	18567.5(8)	8444.7(3)	10729.2(9)	10969(3)
Z	3	2	3	3
ρ_{calc} g/cm^3	0.929	1.361	1.607	1.572
μ /mm^{-1}	8.264	12.113	1.762	13.989
F(000)	5064.0	3376.0	5064.0	5064.0
Crystal size/mm^3	0.1 × 0.09 × 0.06	0.14 × 0.13 × 0.08	0.13 × 0.12 × 0.07	0.12 × 0.1 × 0.08
Radiation	CuKα (λ = 1.54184)	CuKα (λ = 1.54184)	MoKα (λ = 0.71073)	CuKα (λ = 1.54184)
2Θ range for data collection /°	4.66 to 129.984	4.048 to 132.99	4.526 to 52.72	7.032 to 134.986
Index ranges	-51 ≤ h ≤ 46, -36 ≤ k ≤ 51, -5 ≤ l ≤ 12	-29 ≤ h ≤ 13, -14 ≤ k ≤ 29, -16 ≤ l ≤ 18	-24 ≤ h ≤ 31, -31 ≤ k ≤ 26, -23 ≤ l ≤ 24	-15 ⩽ h ⩽ 30, -30 ⩽ k ⩽ 14, -23 ⩽ l ⩽ 23
Reflections collected	46480	26474	21789	7657
Independent reflections	19616 [R_{int} = 0.0648, R_{sigma} = 0.0918]	2773 [R_{int} = 0.0487, R_{sigma} = 0.0275]	2614 [R_{int} = 0.0374, R_{sigma} = 0.0205]	2359 [Rint = 0.0641, Rsigma = 0.0932]
Data/restraints/parameters	19616/2242/1367	2773/195/265	2614/134/244	2359/170/244
Goodness-of-fit on F^2	1.101	1.129	1.125	1.129
Final *R* indexes [I>=2σ (I)]	R_1 = 0.1378, wR_2 = 0.4309	R_1 = 0.0798, wR_2 = 0.2080	R_1 = 0.0529, wR_2 = 0.1553	R_1 = 0.1233, wR_2 = 0.3267
Final *R* indexes [all data]	R_1 = 0.1564, wR_2 = 0.4506	R_1 = 0.0886, wR_2 = 0.2124	R_1 = 0.0673, wR_2 = 0.1654	R_1 = 0.1601, wR_2 = 0.3459
Largest diff. peak/hole / e Å^{-3}	2.25/-3.01	1.40/-1.40	1.22/-0.87	3.10/-0.93

$R_1 = \sum||F_o|-|F_c||/\sum|F_o|$. $wR_2 = [\sum w(F_o^2 - F_c^2)^2/\sum w(F_o^2)^2]^{1/2}$

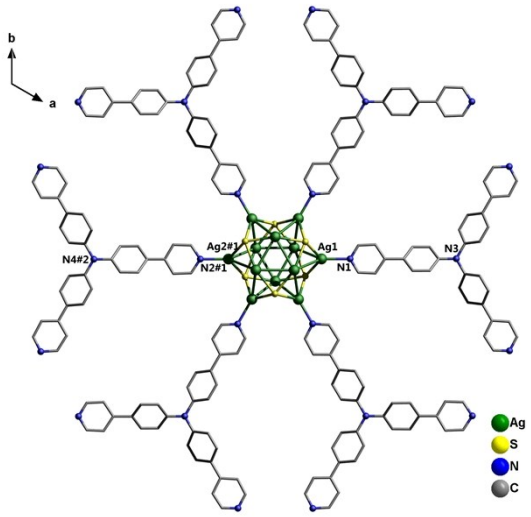

Figure S3. Perspective view of the $Ag_{12}S_6$ node with six pendent TPPA linkers in one layer.

Table S2. Distances (Å) comparison between corresponding atoms in **Ag_{12}TPPA·AA** and **Ag_{12}TPPA·AB** as demonstrated in Figure S3.

	Ag_{12}TPPA·AA	**Ag_{12}TPPA·AB**
Ag1−Ag2#	7.6647(1)	7.5284(15)
Ag1−N1	2.2918(0)	2.273(13)
N1−N2#1	12.2146(1)	12.107(14)
N3−N4#2	29.2640(3)	29.1072(3)

Symmetry codes: #1: *y* −*x* +1 , 1 −*x*, +*z*; #2: *x* −1, *y*, +*z*.

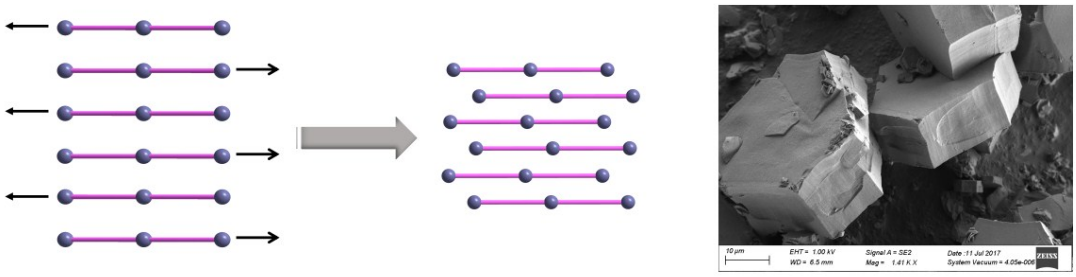

Figure S4. Schematic diagram of **Ag_{12}TPPA·AA** changing to **Ag_{12}TPPA·AB** and SEM image of **Ag_{12}TPPA·AA** grown for two hours and air-dry to **Ag_{12}TPPA·AB**.

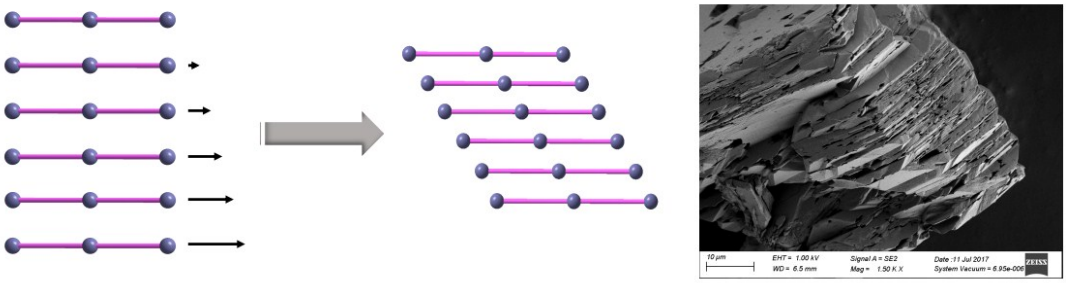

Figure S5. Schematic diagram of **Ag_{12}TPPA·AA** changing to **Ag_{12}TPPA·ABC** and SEM image of **Ag_{12}TPPA·AA** grown for 24 hours and air-dry to **Ag_{12}TPPA·ABC**.

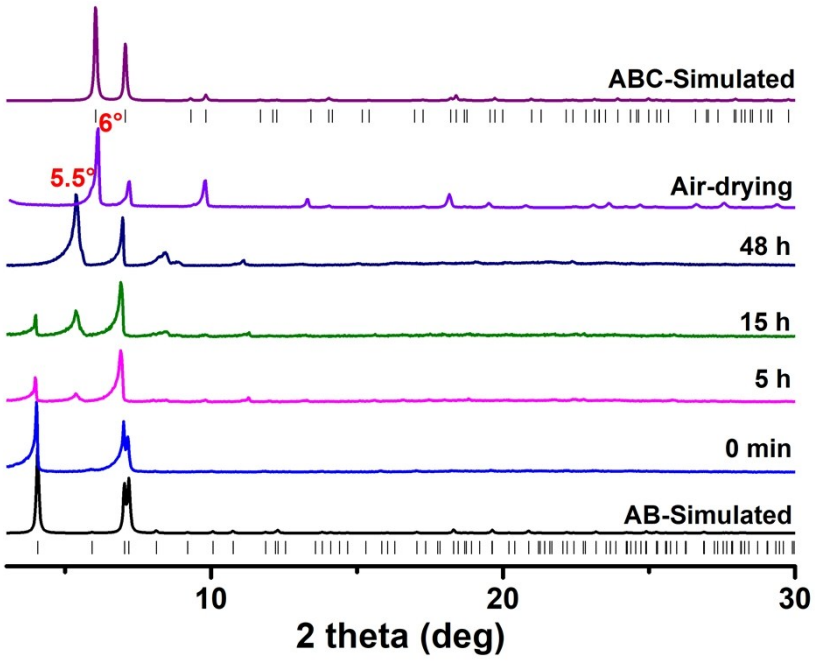

Figure S6. PXRD patterns of **Ag_{12}TPPA·AB** soaked in DMAc and changed to **Ag_{12}TPPA·ABC**.

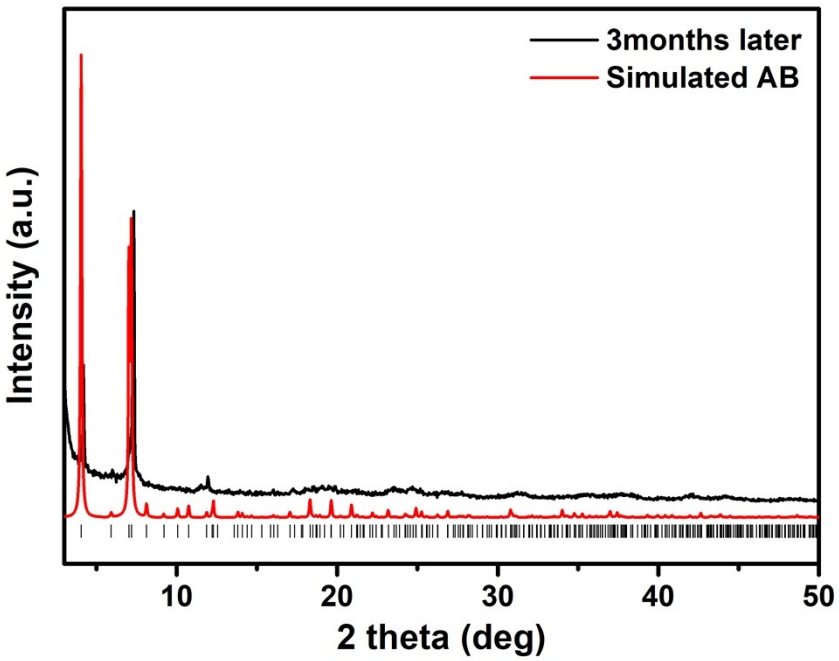

Figure S7. PXRD patterns of **Ag_{12}TPPA·AB** under ambient conditions for 3 months.

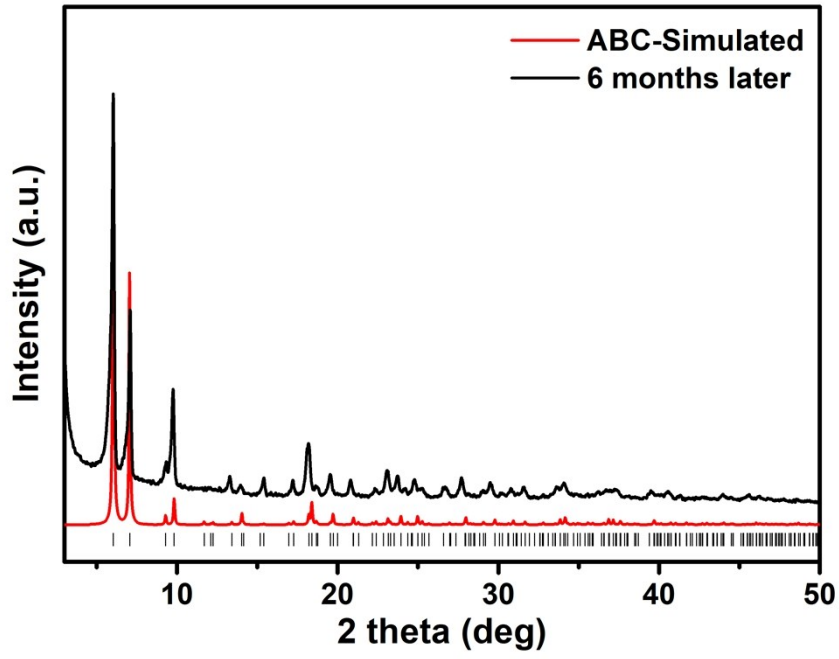

Figure S8. PXRD patterns of **Ag_{12}TPPA·ABC** under ambient conditions for 6 months.

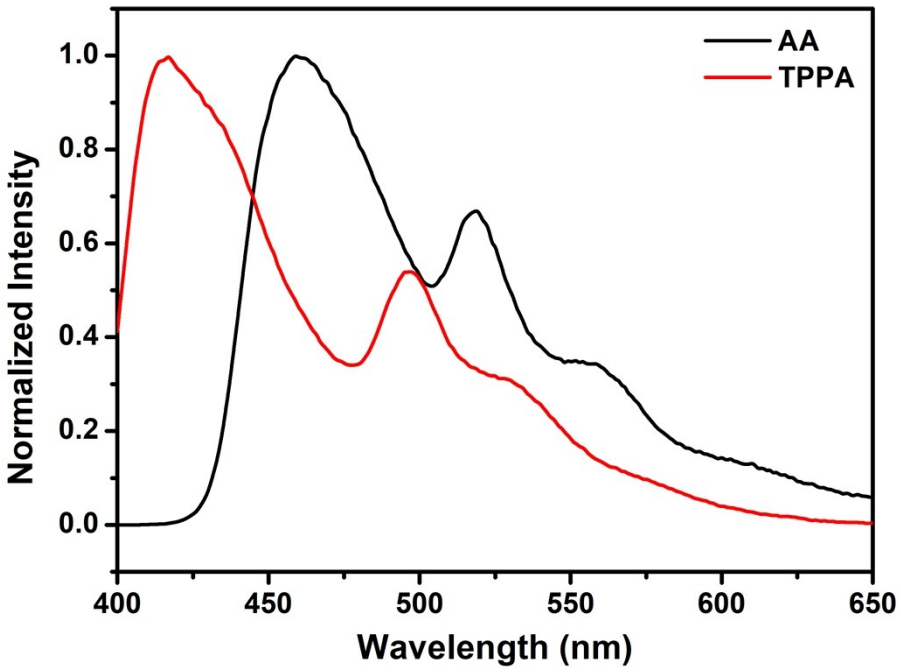

Figure S9. Luminescence spectra of solid **Ag_{12}TPPA·AA** and TPPA in DMAc (10^{-6} M) at 83K upon excitation at 320 nm and 380 nm, respectively.

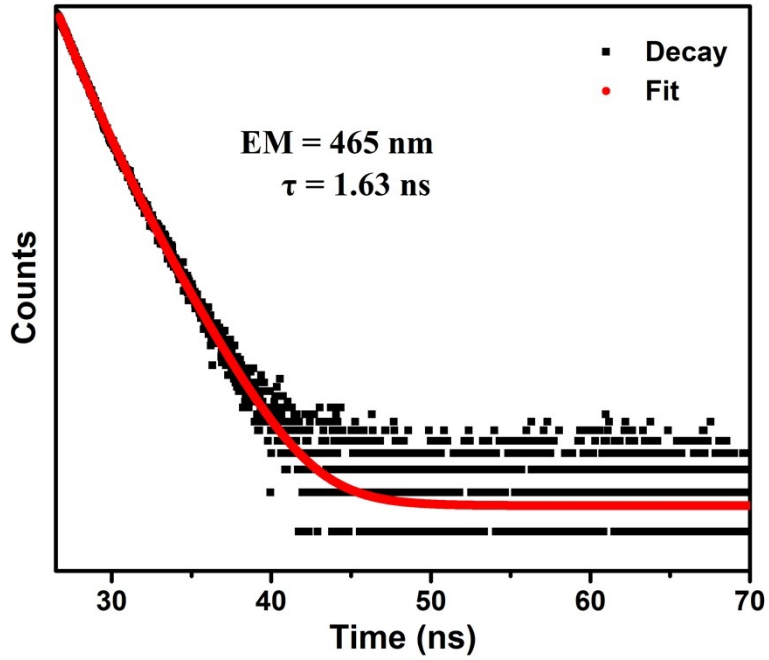

Figure S10. Photoluminescence decay profile of **Ag_{12}TPPA·AA** measured at 465 nm at 83 K using 330 NanoLed.

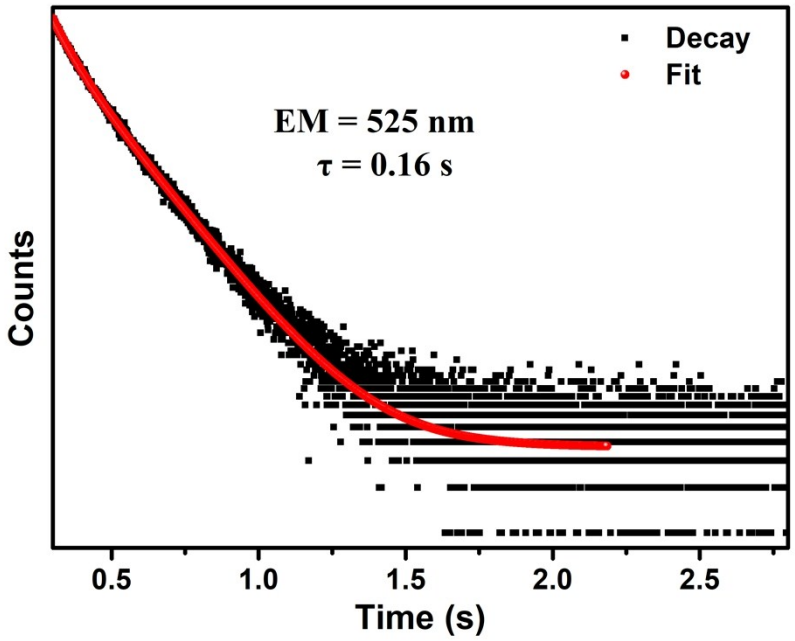

Figure S11. Photoluminescence decay profile of **Ag_{12}TPPA·AA** measured at 525 nm at 83 K using 355 SpectralLed.

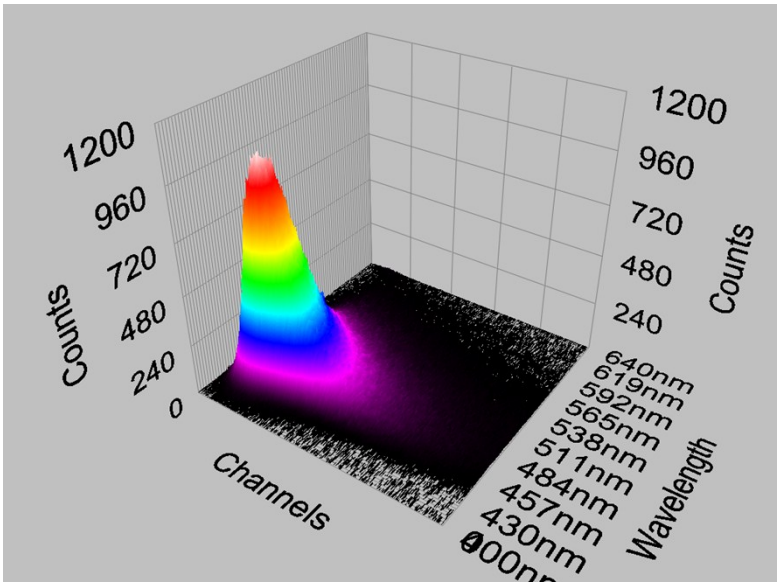

Figure S12. 3D Time-Resolved Emission Spectra (TRES) of **Ag_{12}TPPA·AA** measured at 83 K, the decay measurement range (Channels) was set as 100 ns with the wavelength ranging from 400 to 640 nm using 330 nm NanoLED laser as the excitation light source.

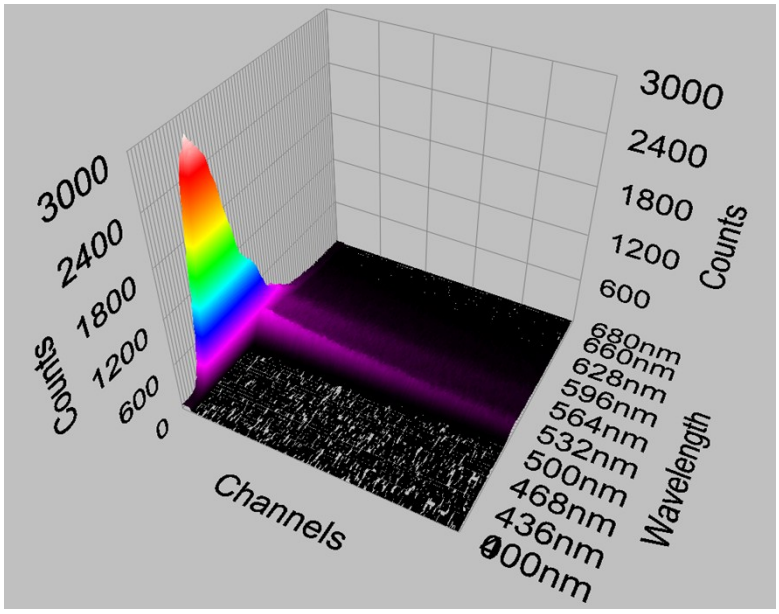

Figure S13. 3D Time-Resolved Emission Spectra (TRES) of **Ag_{12}TPPA·AA** measured at 83 K, the decay measurement range (Channels) was set as 2.8 s with the wavelength ranging from 400 to 680 nm using 355 nm SpectraLED laser as the excitation light source.

References

[1] CrysAlisPro 2012, Agilent Technologies. Version 1.171.36.31.

[2] SCALE3 ABSPACK in CrysAlis PRO.

[3] G. M. Sheldrick, Acta Crystallogr. Sect. A 2015, **71**, 3-8.

[4] G. M. Sheldrick, A short history of SHELX. *Acta Cryst.* A 2008, **64**, 112-122.

[5] O. V. Dolomanov, L. J. Bourhis, R. J. Gildea, J. A. K. Howard, H. Puschmann, OLEX2: a complete structure solution, refinement and analysis program. *J. Appl. Cryst.* 2009, **42**, 339-341.

[6] G. M. Sheldrick, Crystal structure refinement with SHELXL. *Acta Cryst. C* 2015, **71**, 3-8.

[7] M. D. Zhang, C. M. Di, L. Qin, X. Q. Yao, Yi-Zhi Li, Zi-Jian Guo, He-Gen Zheng, *Cryst. Growth Des.*, 2012, **12**, 3957-3963.